Nucl. Sci. and Tech, Vol.5, No. 4 (2015), pp. 01-08

Nuclear Science and Technology

Journal homepage: https://jnst.vn/index.php/nst

Analysis of Containment Pressure and Temperature Changes Following Loss of Coolant Accident (LOCA)

Nguyen Van Thai[1,*], Kieu Ngoc Dung[2]

[1] *School of Nuclear Engineering and Environmental Physics, Hanoi University of Science and Technology*
[2] *Military Institute of Chemistry and Environment*
e-mail: thai.nguyenvan@hust.edu.vn

Abstract: This paper present a preliminary thermal-hydraulics analysis of AP1000 containment following loss of coolant accident events such as double-end cold line break (DECLB) or main steam line break (MSLB) using MELCOR code. A break of this type will produce a rapid depressurization of the reactor pressure vessel (primary system) and release initially high pressure water into the containment followed by a much smaller release of highly superheated steam. The high pressure liquid water will flash and rapidly pressurize the containment building. The performance of passive containment cooling system for steam removal by condensation on large steel containment structure is a major contributing process, controlling the pressure and temperature maximum reached during the accident event. The results are analyzed, discussed and compared with the similar work done by Sandia National Laboratories.

Keywords: *Containment, Pressure, Temperature, LOCA*

I. INTRODUCTION

The passive containment cooling system (PCS) of AP1000 technology is designed such that for all break sizes, up to and including the double-ended severance of a reactor coolant pipe or secondary side pipe, the containment peak pressure is below the design pressure [1]. The energy released to the containment atmosphere following a postulated design basis high energy line break is removed from the exterior containment shell surface by a combination of convection and radiation from dry surface areas and by convection, radiation, and water evaporation from wetted surface areas, to a naturally circulating air stream (Fig. 1). The containment shell outer surface is wetted with water that is stored in a tank located above the containment. Piping and two parallel valves provide a flow path from the tank to the top of the containment shell. The valves open upon receipt of a high pressure signal, allowing water from the tank to drain by gravity through the piping to a central distribution bucket located above the center of the containment shell. This water flow fills the distribution bucket, overflows out onto the dome, and spreads outward on the nearly horizontal surface at the top of the containment shell [3].

Containment code systems have been developed to investigate the complex thermal–hydraulics and their propagation within a containment during accidents. Lumped parameter codes offer the possibility to gain calculation results of postulated accidents within a limited amount of time in the order of hours along with reasonable consistency. The goal of consistent results of calculations is accomplished by the validation of the codes

https://doi.org/10.53747/jnst.v5i4.200
Received 30 September 2015, accepted 23 December 2015

against experimental studies considering a variety of thermal–hydraulic phenomena [4].

The CONTAIN code [5] was developed by SNL and is a specialized computer code used to perform thermal-hydraulic calculations inside containment following a variety of postulated high energy breaks, and serves as a repository of accumulated knowledge in the area of containment analysis technology. CONTAIN, which is the NRC's principal containment analysis tool used to audit industry's safety analysis calculations, incorporates the best current understanding of all relevant phenomena, and has an extensive validation base.

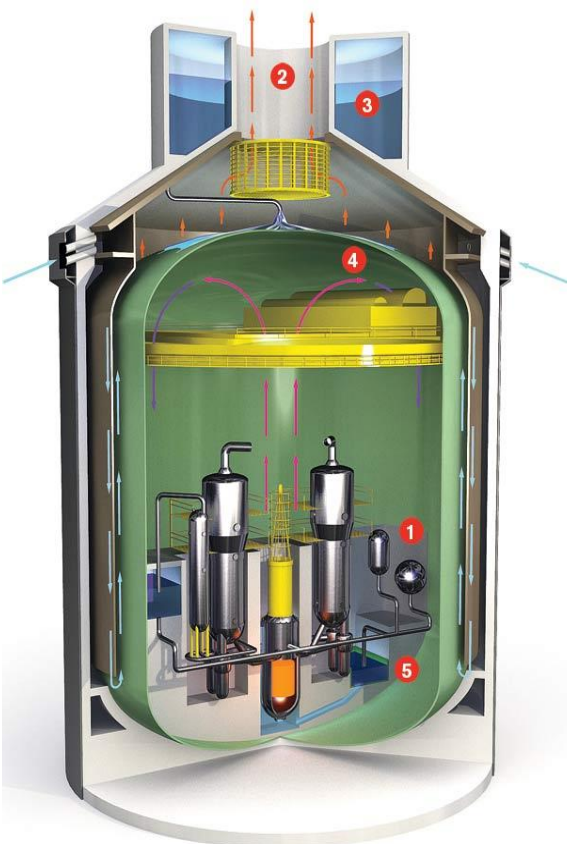

Fig.1. Performance of AP1000 Passive Containment Cooling System [2]

1) As steam escapes, falling pressure within the reactor's pipes causes Core Makeup Tank to send water to the reactor. If the pressure continues to fall, an Accumulator Tank release its contents

2) If the containment grows hotter, it heats the air above it, which exits through an aerial opening, drawing in cool air (blue arrows) from outside

3) Water to cool the containment is drawn down by gravity, eliminating the needs for pumps

4) Rising steam (pink arrows) is cooled and condenses, falling back (purple arrows) to the floor

5) A sump pumps water from the containment floor back into the system. If initial safety measures fail to stabilize the reactor core, the sump works in reverse, flooding the reactor vessel with water

WGOTHIC, COCOSYS, and MELCOR also have been used for peak pressure analysis and assessment of film cooling efficiency [1,4,6,7]. These investigations are based on conservative assumptions which considered an accident scenario for a doubled guillotine break of cold leg.

In the operation of PCS system, the energy removal due to water evaporation dominates the PCS total heat removal and is a function of the PCS flow rate, the wetted area, and the external shell temperature. Since these parameters vary with time, the energy removal rate due to evaporation also varies with time. As the water coverage of the containment shell decreases due to the decrease in the delivered PCS flow rate with time, alternate wet and dry stripes are formed on the containment shell exterior surface and two-dimensional (radial and circumferential) heat conduction is established in the containment shell [3].

Huang and Cheng [7] has pointed out one of the noteworthy phenomena of falling water film in which the evaporation water film is getting thinner as it flows downward on the exterior surface containment. As mentioned in their work, before the water film has been completely evaporated, water film will split into rivulets with the formation of dry patches which could limit the fraction surface covered by film and thus reduce cooling effectiveness.

Moreover, interfacial shear stress at film surface created by the countercurrent natural circulation of gas in PCS channel can change the velocity distribution of the falling film and therefore change the thickness as well as total energy and it may affect the water film cooling effectiveness. This study aims at MELCOR capability of evaluating and quantifying uncertainties of film cooling models. Preliminary assessment results of PCS performance are presented and analyzed.

II. LIQUID FILM MODELING IN MELCOR

Film Models

The mass of a liquid film on a heat structure boundary surface is determined from

(a) calculation of the mass which is transferred between this surface and its boundary volume by condensation, evaporation or draining,

(b) the liquid mass which is transferred to this surface, and

(c) the liquid mass which is transferred to this surface by external sources or film drainage from other heat structure surfaces in film tracking network.

The mass of the liquid film and the film surface and structure surface temperatures enable its thickness and specific enthalpy to be determined. The film equations are nodalized so that half of the film mass is associated with the film/structure interfacial node and the other half is associated with the atmosphere/film interfacial node. Therefore, the average specific enthalpy of the film is given by 0.5 • [$h_f(T_{s,srf})$ + $h_f(T_{f,srf})$], where $h_f(T)$ is the specific enthalpy of the film at temperature T, $T_{s,srf}$ is the film/structure interfacial temperature and $T_{f,srf}$ is the atmosphere/film interfacial temperature [8].

Film Tracking Model

For structures which are part of a film tracking network, the film thickness on a surface is determined iteratively as a function of the Reynolds number of the film flow rate as follows. First, the Reynolds number of the film flow is given by

$$\mathrm{Re}_f = 2(\dot{m}_{in} + \dot{m}_{out})/(w\mu_t) \qquad (1)$$

where $\dot{m}_{in}$ is the mass inflow rate (kg/s) from film drainage to the surface from other surfaces in the network and water deposited on the surface by other MELCOR packages, $\dot{m}_{out}$ is the mass outflow rate (kg/s) from film drainage from this surface (which is to be determined iteratively), w is the width of this surface and μ_t is the bulk viscosity of the film. As an initial guess $\dot{m}_{out}$ is set equal to zero.

The film thickness as a function of Re_f is given by the following correlation

$$\delta_f = C_{f,l} \cdot \delta^* \cdot Re_f^{ef,l} \text{, if } \mathrm{Re}_f < \mathrm{Re}_{LAM}$$

$$\delta_f = C_{f,t} \cdot \delta^* \cdot Re_f^{ef,t} \text{, if } \mathrm{Re}_f > \mathrm{Re}_{TURB} \qquad (3)$$

$$\delta^* = \left[(\mu_f/\rho_f)^2/(g \cdot \sin\theta)\right]^{1/3} \qquad (4)$$

where ρ_f and θ are the film density and angle of inclination of surface from horizontal, respectively.

The film thickness can also be determined from the conservation of film mass as

$$\delta_f = \left[m_{f,0} + (\dot{m}_{in} + \dot{m}_c - \dot{m}_{out}) \cdot \Delta t\right]/(\rho_f A_{srf}) \qquad (5)$$

where $m_{f,0}$ is the film mass at the start of the time step Δt, $\dot{m}_c$ is the condensation rate (a negative value indicates evaporation) and A_{srf} is the surface area. Equation (5) has been presented for the case of rectangular geometry; the equations for cylindrical and spherical geometry are different because the film thickness is related to film volume differently. For given values of $m_{f,0}$, $\dot{m}_{in}$, and $\dot{m}_c$, equations (3) and (5) can be solved simultaneously by iterating on the value of $\dot{m}_{out}$ to determine consistent values of δ_f and $\dot{m}_{out}$ [8].

III. AP1000 PCS NODALIZATION AND BOUNDARY CONDITION SETUP

To build a detailed multi-cell containment model, sufficient design information must be made available from the plant vendor or applicant's design documentation, which typically will include general arrangement drawings of the containment, detailed drawings of specific areas of special interest, other supporting material that defines interconnecting pathways between compartments, and a listing of structural information (concrete, steel-lined concrete, and steel) by location [6]. For the nodalization of the containment, geometry data are obtained from the literature which roughly described general features of AP1000 [4,6,7]. As found by Huang and Cheng [7], the deviation of pressure responses prediction may due to the inevitable discrepancies of containment geometry as well as boundary conditions. The nodalization scheme was shown in Fig. 2.

The region below the operating deck was divided into six regions (301, 302, 303, 304, 305, 306) which are exactly the same with nodalization scheme used in Tills et al (2009) [6]. However, the region above the operating deck was divided into 21 regions instead of 8 regions used in Tills et al. (2009) [6] in order to capture in more details about the mixing of gases within the containment. The issue of regional gas mixing affecting passive heat sink energy transfer was important due to the absence of any active Engineered Safety Features [6].

Table I. AP1000 DECLB LOCA Chronology

			Time (s)	
BLOWDOWN		BREAK OCCURS	0.0	Mass & Energy released into containment
		REACTOR TRIP (PRESSURIZER PRESSURE OR HIGH CONT. PRESSURE)	~2.2	
		SI SIGNAL (HIGH CONT. PRESSURE)	~2.2	
		CMT INJECTION BEGINS	~4.2	
		ACCUMULATOR INJECTION BEGINS	~12	
		END OF BLOWDOWN	~34.5	
	REFIL	BOTTOM OF CORE UNCOVERY	54.0	
REFLOOD		CALCULATED PCT OCCURS	~65	
		ACCUMMULATORS EMPTY: CMT INJECTION COMMENCES AGAIN	~150	
LONG TERM COOLING		ADS ACTIVATES ON LOW CMT LEVEL SIGNALS/IRWST ACTIVATES	~1500	Mass & Energy released into containment
		IRWST EMPTY: COOLING CONTINUES VIA CIRCULATION OF SUMP WATER		

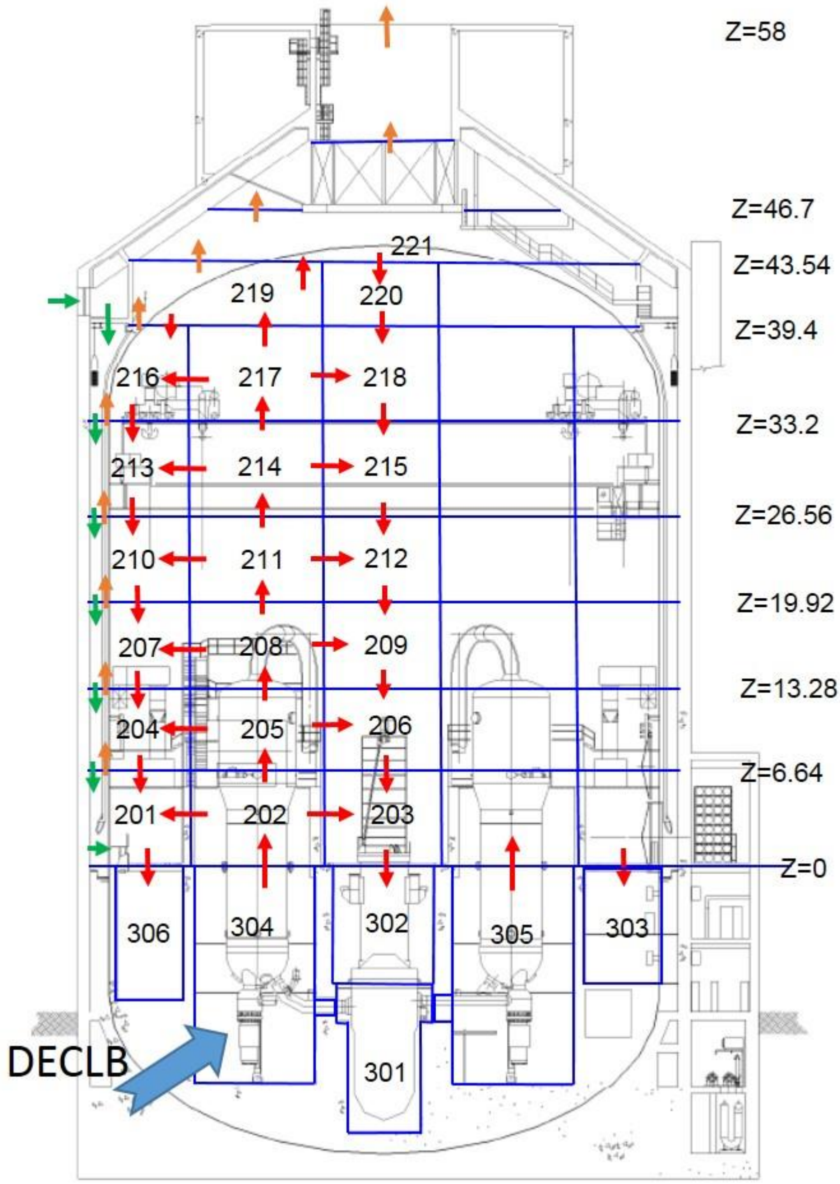

Fig.2. Nodalization scheme of AP1000

The AP1000 DECLB LOCA chronology is shown in Table I. The mass and energy released into the containment for the DECLB scenario can be found in AP1000 Design Control Document and plotted in Fig. 3 and 4.

During the first phase of blowdown, a two-phase flow of water from the vessel side and steam from the steam generator side is released into the containment via the break flow deck at the bottom of the East steam generator compartment. After the blowdown phase the reflooding of the reactor begins with water injection from the accumulators (ACC) and this injection is switched to core-makeup tank (CMT) between 200~250 seconds. When the water level in CMT is lower than the setpoint level, water injection from In-Containment Refueling Water Storage Tank to the reactor starts and the automatic depressurization system (ADS) valves of the steam generators are opened and steam is released equally into both upper SG compartments.

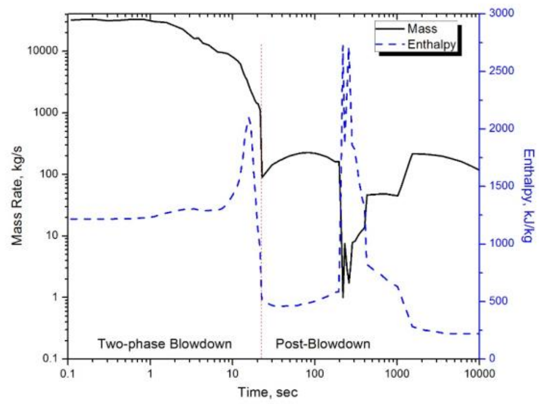

Fig.3. Two-phase water released to Containment for DECLB LOCA (vessel side break flow)

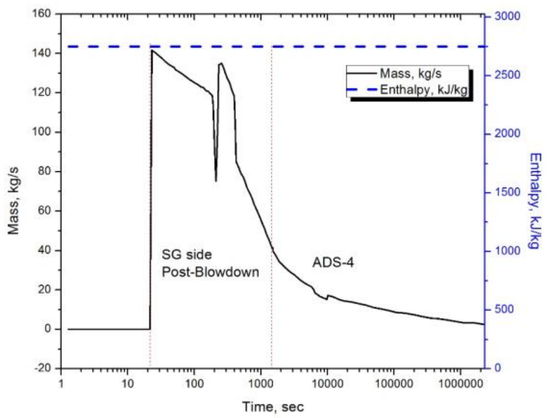

Fig.4. Steam injections into the AP1000 steam generator compartments, post-blowdown and ADS-4 (both two loops)

The water flow rate for flooding the containment outer shell is shown in Fig. 5. The flooding is introduced at the top of the shell, and through a weir setup distributed in a nearly uniform manner to the shell with wetted coverage of 90% (Tills et al., 2009)

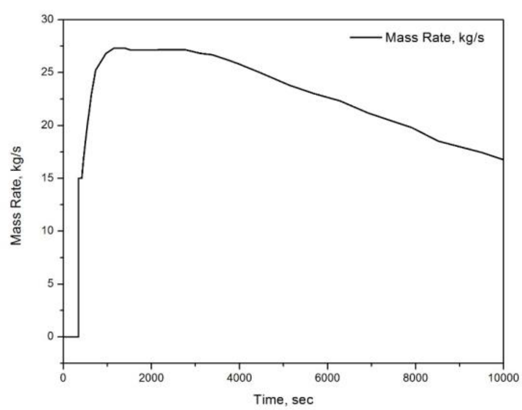

Fig.5. Outer containment shell water flood rate for PCS

IV. RESULTS AND DISCUSSION

The AP1000 containment integrity analysis assumed the same conservative steam generator energy release rates as conventional plants (Fig. 4). This assumption resulted in a double-peaked pressure response curve; the first peak resulting from the initial blow down of Reactor Cooling System (RCS), and the second peak resulting from arbitrarily rapid release of the steam generator energy.

Comparions of MELCOR calculated long-term pressure profiles during AP1000 DECLB LOCA are shown in Fig. 6. Because the blowdown process is so rapid, the pressurization is nearly adiabatic and pressure response peak is limited through the accommodation of the blowdown steam in the containment free volume. The free volume of 58,330 m^3 was used in most calculations resulting in the same predicted value of the first pressure response peak. The progress of containment pressurization in post-blowdown phase significantly depends on the performance of PCS, heat structures as well as the amount and distribution of short-term heat sinks (metal from equipment, components, and structures) in the compartments.

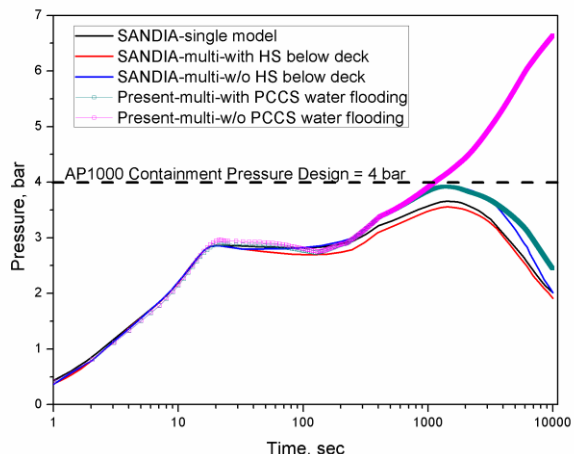

Fig. 6. Comparison of MELCOR-calculated long-term pressure profiles during AP1000 LOCA event

As can be seen in Fig. 6, in case of PCS water not injected on the top of containment outer surface, the pressure inside containment is continuously increased and become larger than design value (~ 4 bar) which may lead to containment failure. When the PCS works correctly as designed, the second peak pressure is reached at about 1500 seconds. The calculated pressures in this study are comparable with the results done in SANDIA Laboratory [6]. Of course, the deviations are accounted for the nodalization scheme, containment geometry and amount of heat structures in the compartments.

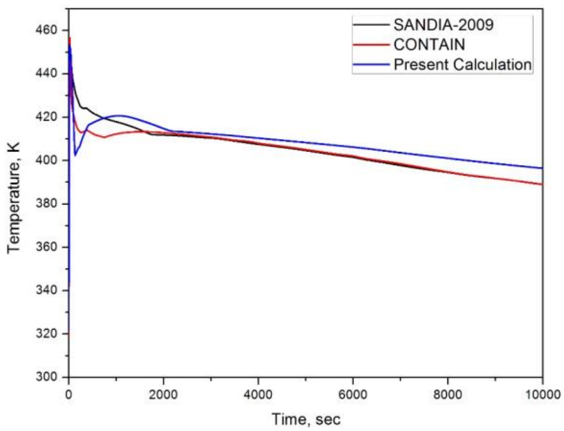

Fig.7. Comparison of MELCOR-calculated long-term gas temperature in region above the deck

Comparisons of temperature calculated above the operation deck, where the maximum temperatures occur as shown in Fig. 7 during the long-term of AP1000 DECLB LOCA. The comparisons indicate that long term trend toward saturation for all calculations. However, deviations are found shortly after the blowdown period when maximum temperatures above deck occur. It may account for mixing phenomena inside the containment since the region above operation deck are divided into 21 control volumes in this study, while 8 control volumes have been used in the calculations with CONTAIN and MELCOR at SANDIA Lab. It is also interesting to note that the prediction results are different with MELCOR and CONTAIN codes even the same nodalization scheme has been used. It can be explained in such way that the differences in the blowdown period heat removal rates in the above and below operating deck regions may account for the mixing effects inside the containment. These differences are due to a variance between calculations in the steam flow splits among the various pathways exiting the break room during a period of rapid phase separation and disposition in the break room, and the manner in which condensate accumulation on structures is treated within each code [6] .

Figure 8 showed film thickness calculations for specific area locations along the shell exterior surface (8 segments). Flooding of the shell begins at 341.0 seconds. The film thickness was calculated based on film tracking model mentioned in Section II. It is shown that there is 100% evaporation of PCS flood water at the time (~7500 seconds). Tills et al. (2009) [6] reported that PCS flood water are evaporated 100% at the time (~1500 seconds) when the maximum containment pressure load occurs. From the results of film mass calculations presented in their report [6], however, the time should be the same with our calculation. Fortunately, this fact was confirmed from Figure 3.18 in their report.

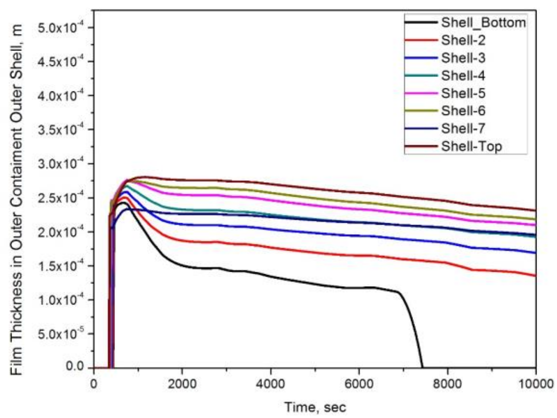

Fig.8. Water film thickness on the containment outer surface

A comparison of exit air flow velocity from the PCS duct is shown in Fig. 9. It can be seen that the prediction result of air rise velocity at the exit of PCS is higher in comparison to that performed in SANDIA Lab. It should be noted that the passive heat removal mechanism maintained inside the downcomer and riser regions strongly depends upon air temperature at the inlet and outlet of PCS system as well as its geometry configuration. This detailed information was not provided in DCD documents as well as SANDIA Lab's calculations and which may accounts for the deviations. The sensitivity and uncertainty studies on air temperature and geometry configuration will be included in the near future work.

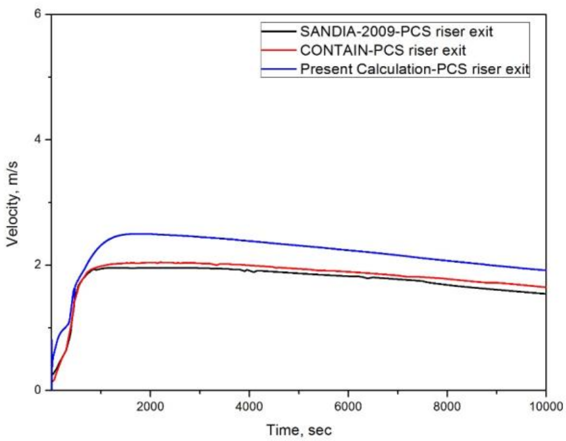

Fig.9. Air velocities in the PCS riser exit during AP1000 DECLB LOCA event

V. CONCLUSIONS

Preliminary simulations of AP1000 PCS performance have been carried out using MELCOR 1.8.6 code. It has been shown that the MELCOR code is applicable to predict the maximum containment loads with a multi-cell containment during AP1000 DECLB LOCA event. Similar results are obtained compared with works done in SANDIA Laboratory. Future works would focus on evaluating and quantifying uncertainties of film cooling models.

ACKNOWLEGEMENTS

This work has been supported from Ministry of Science and Technology (MOST) through the National R&D Project: "Study the Nuclear Power Plant’s Technology proposed for NinhThuan 1 and NinhThuan 2 in order to support Basic Design’s Review", code KC.05.26/11-15.

REFERENCES

[1] AP1000 DCD, Nuclear Regulatory Commission, Rev. 19.

[2] R. Edwards, “MIT Technology Review: New Nukes”, 2008.

[3] WCAP-15862, “WGOTHIC Application to AP600 and AP1000”, 2004.

[4] P. Broxtermann, H-J. Allelein, “Simulation of AP1000’s passive containment cooling with the German Containment Code System COCOSYS”, Nuclear Engineering and Design 261, pp. 326-332, 2013.

[5] K.K. Murata et al., “Code Manual for CONTAIN 2.0: A Computer Code for Nuclear Reactor Containment Analysis,” NUREG/CR-6533, SAND-1735, Sandia National Laboratories, Albuquerque, NM, December 1997.

[6] J. Tills, A. Notafrancesco, and J. Phillips, “Application of the MELCOR Code to Design Basic PWR Large Dry Containment Analysis”, SANDIA report, SAND2009-2858, 2009.

[7] X. Huang and X. Cheng, “Modification and application of water film model in COCOSYS for PWR’s passive containment cooling”, Nuclear Engineering and Design 280, pp. 251-261, 2014.

[8] MELCOR Computer Code Manuals, NUREG/CR-6119, SAND2000-2417.